# Thundercloud Electrification: Cloud Growth and Electrical Development

AMI ZIV AND ZEV LEVIN

*Dept. of Environmental Sciences, Tel-Aviv University, Ramat Aviv, Israel*

(Manuscript received 24 November 1973, in revised form 29 March 1974)

ABSTRACT

A time-dependent numerical model is used to simulate the growth of the electric field in thunderclouds by the polarization mechanism, including both the growth of hydrometeors and the growth of the electric charge centers. The results demonstrate a direct coupling between the hydrometeor growth and the electric field. Different types of cloud are discussed with reference to their electrical behavior.

It is found that clouds containing large ice particles and small supercooled water drops and fully glaciated clouds can produce electric fields sufficient for lightning to occur. Electrical forces in the clouds tend to slow down the relative fall velocities of the precipitation particles, and reduce their interaction rate. The net effect is a slowing down of the growth of the hydrometeors and the rate of buildup of the electric field.

## 1. Introduction

The phenomena of cloud electrification have been discussed in the literature for a long time and many mechanisms have been proposed to explain all or part of the charges generated during the lifetime of thunderclouds. Many of them either do not satisfy the necessary requirements of the electrification process (Mason, 1971) or they require special conditions which are not always prevalent in electrified clouds. Recently, however, it was demonstrated both theoretically (Sartor, 1970; Mason, 1972) and experimentally (Scott and Levin, 1970; Levin and Hobbs, 1971; Aufdermaur and Johnson, 1972) that the primary aspects of charge generation in clouds can be explained by the polarization charging mechanism.

This charging process is a result of collisions and separations of particles of different fall velocities in the presence of an ambient electric field. Fig. 1 illustrates a sequence of events during the polarization charging of cloud particles. Laboratory and field experiments have indicated that such collisions can separate charges in amounts comparable to theoretical expectations though some measured values of charge have actually exceeded theoretically predicted values.

Recently, two theoretical models have been used to investigate the growth of the electric field by this process (Sartor, 1967, 1970; Mason, 1972). Sartor considers only the growth of the electric field without allowing the cloud particles to grow and without considering the effect of the electrical forces on the particles. Mason considers interactions between the growth of particles and the electric field but constrains the liquid water to an arbitrary exponential form. In addition, Mason computes the accumulated charge on the precipitation and cloud particles assuming that the electric field is time-invariant. Recently, Paluch and Sartor (1973) have extended Sartor's (1970) model to account for the fact that the values of the electric field during each interaction is determined by the previous interaction. However, they too do not allow any growth of the hydrometeors to take place.

This work seeks to provide a more realistic treatment utilizing an extended size distribution in a fully

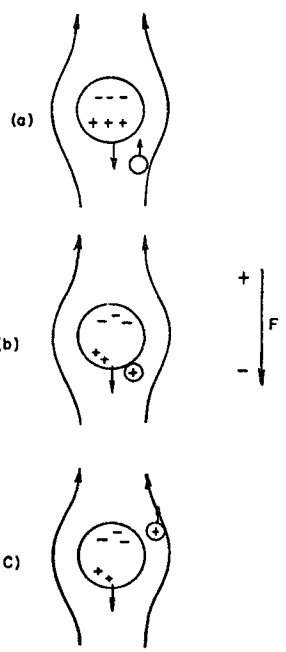


FIG. 1. Sequence of events during the polarization charging of cloud particles.

Unauthenticated | Downloaded 06/25/24 06:41 PM UTC

time-dependent framework, including 1) the growth of the hydrometeors and the time-dependence of the cloud-water, rainwater size distributions; 2) the variation of charges on the hydrometeors with time; and 3) the growth of the electric field.

## 2. The model

To characterize the interactions among particles in a cloud it is assumed that the initial size distribution (to be discussed later) has formed by the time the calculations begin. This initial size distribution then changes as the particles interact and grow. The cloud itself is considered as a whole, and is pictured as a parallel plate capacitor without horizontal gradient, a uniform vertical electric field, a uniform distribution of particles, and only an implicit vertical dimension. Within the cloud volume, particles of a given size become charged through interactions and polarization charging.

In essence, our picture is similar to the simple parallel-plate capacitor model of Sartor except that full interactions are allowed. However, it is also presumed that the cloud is maintained from below by a sustained source so that the falling particles fall through an environment of freshly replenished cloud. Thus, the larger hydrometeors fall through an environment that has a constant concentration of cloud droplets and cloud water content. These larger precipitation particles continuously increase in size by collection of the cloud particles. Some of these interactions result in collisions and then separation, and hence in charge separation.

## 3. The growth of the electric field

Specifically, we consider a 1 cm$^2$ cross section within the horizontal plane and allow the particles to fall vertically under the influence of gravity and electrical forces. The particle interactions act as a current source $\nabla\cdot\mathbf{J}$. The $n_i$ particles each with charge $Q_i$ move with velocities $\mathbf{V}_i$ to produce the source current

$$\mathbf{J}=\sum_i n_iQ_i\mathbf{V}_i, \tag{1}$$

where the summation is over $i$ particle categories. Considering the discharge current $j$, the time rate of change of the charge density $\rho$ is given by considering the continuity of electric charge:

$$\frac{\partial\rho}{\partial t}+\nabla\cdot\mathbf{J}+\nabla\cdot\mathbf{j}=0. \tag{2}$$

Also, since the dielectric constant is approximately unity, Gauss' theorem is simply

$$\nabla\cdot\mathbf{F}=4\pi\rho, \tag{3}$$

where $\mathbf{F}$ is the electric field. Further, Eqs. (1) and (2) can be combined with the differential form of Eq. (3). Then, if the order of differentiation is interchanged, we obtain generalized equation

$$\nabla\cdot\left(\frac{1}{4\pi}\frac{\partial\mathbf{F}}{\partial t}+\sum_i n_iQ_i\mathbf{V}_i+\mathbf{j}\right)=0. \tag{4}$$

(This form is obtainable from Maxwell's equations if magnetic effects are ignored.) Also imposing the restrictions of horizontal homogeneity, and no initia electric charges or initial variations in the electric field the equation of Mason (1972) results:

$$\frac{dF}{dt}=-4\pi\left(\sum_i n_iQ_iV_i+j\right). \tag{5}$$

The discharge currents consist of two parts: 1) linear currents $(-\lambda F)$ where $\lambda$ is the electrical conductivity and 2) currents not linear to the field, e.g., point discharge currents. To account for both of these discharge currents, nonlinear expressions for $J$ as a function of $F$ were used by Sartor and Mason. Sartor used the first two terms of a polynomial. Mason used an exponential form to fit the two points: (i) cloudy air at 5 km with $\lambda=2\times10^{-4}$ esu, and (ii) cloudy air in the presence of a high electric field with $\lambda=6\times10^{-4}$ esu. His final empirical equation for $j$ was

$$j=-10^{-3}(e^{0.2F}-1). \tag{6}$$

For lack of better results the present model uses this expression.

## 4. The charge transfer equations

Expressions for the charge transferred as a result of collisions of conducting rigid spheres were first presented by Latham and Mason (1962). Davis (1964) has since presented a numerical solution with full detail. His solutions to the charge transferred by the interacting particles can be written in a modified form:

$$\Delta Q_{ij}=\Phi FR_i^2\cos\theta+(\omega-1)Q_j+\omega Q_i, \tag{7}$$

where

$$\omega=\frac{A_2}{A_2-A_1},\quad \phi=\frac{A_3}{A_2-A_1}, \tag{8}$$

and $A_l$ ($l=1, 2, 3$) are Davis' tabulated coefficients. (Table 1 presents the values of $\omega$ and $\phi$ for different ratios of the radii of the interacting particles.) In (7) $Q_j$ is the initial charge on the large particle prior to collision, $Q_i$ the initial charge on the small particle, $\Delta Q_{ij}$ the charge transferred to the large particle as a result of the collision, and $\theta$ the angle between the line connecting the centers of the particles and the electric field. (The subscripts $i$, $j$, $k$ represent the relative size of the different particles where particle $i$ is smaller than $j$ which is smaller than $k$.)

Unauthenticated | Downloaded 06/25/24 06:41 PM UTC

TABLE 1. Values of $\phi$ and $\omega$ (see text).

| $r/R$ | 1 | 0.8 | 0.6 | 0.5 | 0.4 | 0.2 | 0.1 | 0 | Source |
|---|---|---|---|---|---|---|---|---|---|
| $\phi$ | 1.62 | — | — | 2.80 | — | 4.0 | 4.57 | — | Sartor (1970) and Davis (1964) |
| $\omega$ | 0.50 | 0.60 | 0.714 | 0.775 | 0.838 | 0.948 | 0.985 | 1.00 | The present work |

In many cases, however, the cloud particles are not good conductors and the time of contact of the particles is too short for all the available charge to be transferred. This effect is taken into account by the addition of the term $(1-e^{-t_c/\tau})$ which compensates for the lack of time for relaxation of the electrical charge. Here $t_c$ is the time the particles are in contact before separation, and $\tau$ is the relaxation time of the charge carriers [$\tau=\epsilon/(4\pi K)$, where $\epsilon$ is the dielectric constant and $K$ the electrical conductivity of the particles] which is a function of temperature. The contribution of this product may become important for ice at temperatures lower than about $-10$C, since at that temperature $\tau$ is of the order of $10^{-3}$ sec (see Sartor, 1970) which is comparable to the value of $t_c$ (Scott and Levin, 1970).

The resulting equation for the charge transferred upon a collision is

$$\Delta Q_{ij}=[\phi F R_i^2\cos\theta+(\omega-1)Q_j+\omega Q_i](1-e^{-t_c/\tau}). \quad (9)$$

## 5. The accumulation of charge and the growth of the electric field

Assume that the particles are separated into $N$ size intervals. The particles move vertically and separate charges which are continually being drained by the vertical discharge currents. Looking at a cylindrical column of unit cross section in the middle of the active part of the cloud, we see that the total positive charge that a cloud particle of radius $R_j$ receives in time $dt$ by collisions with particles larger than itself is

$$\tfrac{1}{2}\pi\sum_{k=j+1}^{N}(R_j+R_k)^2(V_k-V_j)n_kE_1(j,k)E_2'(j,k)\Delta Q_{jk}, \quad (10)$$

where $\Delta Q_{jk}$ is given by Eq. (9); $V_j$ and $V_k$ are the terminal velocities of particles of radii $R_j$ and $R_k$ respectively, $n_k$ is the concentration of particles of size $k$, $E_1(j,k)$ the collision efficiency of particles with radii $R_j$ and $R_k$, and $E_2'(j,k)$ the efficiency of partial coalescence.

In Eq. (10) the constant $\frac{1}{2}$ provides for the lack of collisions involving the smaller particles which are "upstream" of the larger particles (following Sartor, 1967). This is demonstrated schematically in Fig. 2. Here we see three columns, each representing the location of the given particle class. The particles are pictured as starting their fall at a given time from the starting line. We see that particles of size $R_j$ present above line A do not collide with larger particles $R_K$.

A similar expression can be derived for the total charge taken away from a particle of radius $R_j$ by collisions with smaller particles of radius $R_i$. In this equation, however, the constant $\frac{1}{2}$ does not appear since all the smaller particles are involved in the collisions. Therefore, the rate of total charge transferred to the $j$th particle is

$$\frac{dQ_j}{dt}=\pi\Big[\tfrac{1}{2}\sum_{k=j+1}^{N}(R_j+R_k)^2(V_k-V_j)n_kE_1(j,k)\times E_2'(j,k)\Delta Q_{j,k}-\sum_{i=1}^{j-1}(R_i+R_j)^2(V_j-V_i)\times n_iE_1(i,j)E_2'(i,j)\Delta Q_{i,j}\Big]. \quad (11)$$

Note the effective interactions that are predicted by Eq. (11) between the two extreme particle categories: the smaller cloud particles, category 1, and the largest precipitation particle, category $N$. The cloud particles lose no charge to smaller particles and they receive almost no charge from the precipitation particles because $n_N$ is relatively small. On the other hand, the precipitation particles gain no charge from larger particles but gain (lose) large amounts of negative (positive) charge from the cloud particles because $n_1$ is relatively large. Simply stated, there are so many more cloud particles than precipitation particles that large charges are accumulated on the precipitation particles through multiple interactions. However, the number of cloud particles is so large that a single particle is unlikely to undergo more than one collision and so acquires a negligible charge.

The net flux of positive current which contributes to the buildup of the electric field is

$$\mathbf{J}=\sum_{i=1}^{N}n_iQ_i\mathbf{V}_i.$$

The cloud is initially uncharged and the interactions of the particles merely separates charges, conserving the total charge. This means that at all times

$$\sum_{i=1}^{N}n_iQ_i=0.$$

As a result, the current flux is independent of the updraft and only the relative velocities of the particles are important, since

$$\sum n_iQ_i(V_i+V_0)=\sum_{i=2}^{N}n_iQ_iV_i+V_0\sum_{i=1}^{N}n_iQ_i, \quad (12)$$

Unauthenticated | Downloaded 06/25/24 06:41 PM UTC

where $V_0$ is any superimposed mean velocity. In the present work the $V_i$ are all terminal velocities and $V_0$ is taken as $-V_1$, the terminal velocity of the smallest particles. This means that

$$\sum_{\text{all particles}} nQV = \sum_{i=2}^{N} n_i Q_i (V_i - V_1), \tag{13}$$

and the velocity reference is the fall velocity of the smallest particles, particles which approximately follow the updraft. It follows that, for unit cross-sectional area, the rate of accumulation of positive (negative) charge on the top (bottom) of the cloud parcel is

$$\frac{dQ}{dt} = \sum_{i=2}^{N} n_i Q_i (V_i - V_1),$$

when the charge centers in the top and bottom of the cloud also follow the updraft or remain in the top and bottom of the cloud parcel.

The final equation for the growth rate of the electric field is obtained by combining Eqs. (5) and (13):

$$\frac{dF}{dt} = -4\pi \Big[ \sum_{i=2}^{N \geq 2} n_i Q_i (V_i - V_1) + j \Big]. \tag{14}$$

## 6. The size distribution

Hydrometeor size distributions and their variation with time in clouds have been intensively investigated both by direct experimental measurements and by numerical models. At this time, it is generally believed that cloud particles grow up to about 20 $\mu$m by condensation after which time autoconversion of the cloud droplets becomes the dominating process in their growth. Models describing the stochastic nature of this process have been published by Golovin (1963), Scott (1968), Slinn and Gibbs (1971), Twomey (1966), Berry (1967), and Kovetz and Olund (1969). Often it is found that in young clouds the concentration of particles decreases approximately in an exponential fashion with radius from a lower radius limit of about 10 $\mu$m. Thereafter, with the onset of autoconversion, the distribution develops a "hump" which eventually develops into rain. To simulate these processes a logarithmic cloud droplet distribution has been combined with a Gaussian form for incipient rainwater. Fig. 3a illustrates the particle mass distribution that is expected; it has a single maximum around particle mass $M_1$ for young clouds (curve 1). But for more mature clouds another peak appears around $M_4$ (curve 2), where $M_4$ represents the mean mass of the precipitation elements. Each peak is approximated by a Gaussian when plotted as a function of radius (Slinn and Gibbs, 1971). As the cloud matures $M_4$ moves to the right while maintaining a Gaussian shape.

In our model the size distribution is approximated by five size intervals: Interval 1 contains the peak at $M_1$ where all the liquid water content of the *cloud particles* is concentrated. Interval 4 contains the peak at $M_4$ of the *precipitation particles* and where one-half the liquid water content of the precipitation portion is concentrated. Intervals 3 and 5 on both sides of $M_4$ (the standard deviation is taken as $0.5M_4$) contain one-fourth of the precipitation liquid water content. Inter-

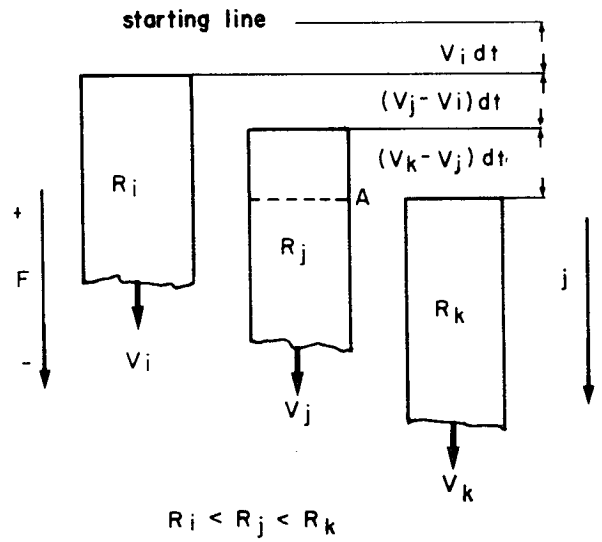


FIG. 2. A schematic diagram of the present model.

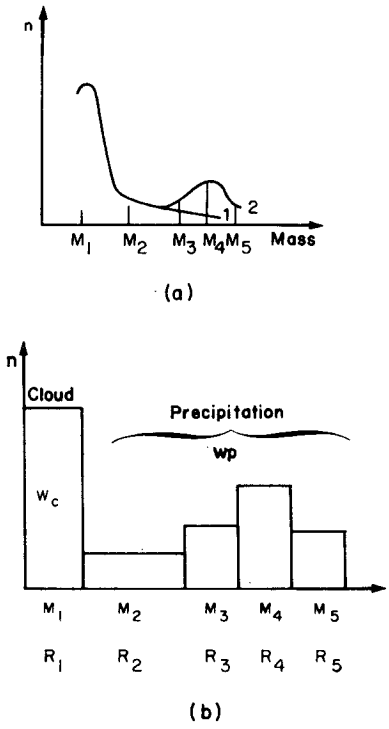


FIG. 3a. Typical mass distributions of particles in a young cloud (curve 1) and in a mature cloud (curve 2). 3b. Mass distribution of the particles in the present model.

Unauthenticated | Downloaded 06/25/24 06:41 PM UTC

val 2 contains the intermediate particle sizes and smooths the gap between $R_1$ and $R_3$. It is computed as a geometrical average between $R_1$ and $R_3$. We compute $n_2$ by a logarithmic interpolation of $n_4$, $n_3$ and $n_1$. The histograms of sizes used in the model is presented in Fig. 3b.

## 7. The growth of the hydrometeors

The precipitation particles grow continuously from collected cloud particles. Specifically, size interval 4 grows in mass according as

$$\frac{dM_4}{dt}=\pi(R_1+R_4)^2(V_4-V_1)n_1M_1E_1(1,4)E_2(1,4), \quad (15)$$

and in radius according as

$$\frac{dR_4}{dt}=\frac{\pi}{3\rho_p}\left(\frac{R_1+R_4}{R_4}\right)^2(V_4-V_1)n_1R_1^3E_1(1,4)E_2(1,4). \quad (16)$$

With the growth of $R_4$ as a function of time, $R_2$, $R_3$ and $R_5$ increase in a prescribed way by addition of liquid water to maintain the Gaussian distribution. The addition of interval 2 to the computations somewhat compensates for the use of the continuous growth process that is slower than a stochastic process which tends to better simulate the real situation (Mason, 1971).

The model evolves with stable, constant properties of the cloud particles (size interval 1). Initially, the sizes and liquid water content of both the cloud particles and the precipitation particles are specified. Then the precipitation particles evolve in time by collection while the cloud particles remain constant in size and maintain a constant liquid water content. The model is simple for numerical calculations, but nonetheless it follows relatively closely the results available in the literature by empirically maintaining the pseudo-Gaussian distribution about $R_4$. At this stage in the development there is certainly no justification for the use of more complicated models which themselves fail to explain the processes of precipitation formation satisfactorily.

In this model electric forces affect the terminal velocities of the particles and the effective precipitation rates [see Eq. (18)]. The method for computing the velocities of the particles is discussed in the Appendix. Considering the terminal velocities of ice crystals, Heymsfield's (1972) data (see Table 2) suggest that the fall velocities of disks and columns are not much different from the fall velocities of spheres of the same mass and density. Also, since cloud ice particles have velocities much lower than the fallspeeds of the precipitation elements, and only the difference in fallspeeds enters the equations, the results are insensitive to the terminal velocity of the ice particles. Therefore, in this treatment the ice particles are considered as spheres with a density of 0.6 gm cm$^{-3}$.

In essence, the liquid water content of the cloud particles is given by $W_c=W_1=n_1M_1$ and that of all precipitation elements by

$$W_p=\sum_{i=2}^{5}W_i=\sum_{i=2}^{5}n_iM_i. \quad (17)$$

The effective precipitation rate is given by

$$p=\sum_{i=2}^{5}n_iM_iV_i=\sum_{i=2}^{5}W_iV_i. \quad (18)$$

## 8. The collision, coalescence, separation, and partial coalescence efficiencies

The collision efficiencies $E_1$ used in the computations are based on the calculated values of Davis and Sartor (1967) as presented in an empirical form by Scott and Chen (1970)[1]. The coalescence efficiencies $E_2$ are calculated by the simple expression recently obtained by Whelpdale and List (1971); they are used to compute the efficiency of coalescence after collision has occurred. Then $(1-E_2)$ expresses the probability that colliding particles will not coalesce. Also, of all the particles that collide, some will make contact or partially coalesce but not merge and proceed to separate. These interactions are of prime interest here because they cause the charge separation. The corresponding partial coalescence $E_2'$ is

$$E_2'=(1-E_2)E_3, \quad (19)$$

where $E_3$ is the efficiency of separation. The possibility of charge transfer by conduction through the air is not considered nor is increased coalescence and collision efficiencies in the presence of high electric fields. An increased value of $E_2'$ (or $E_3$) would tend to increase the charging rate while increased coalescence would tend to decrease $E_2'$, following Eq. (19).

## 9. The numerical method

The growth of charge on particles in a size interval [Eq. (12)] is represented by a first-order differential equation so that $N$ intervals in the size distribution are represented by $N$ such equations. The growth of the electric field is represented by Eq. (14) and the growth of the hydrometeors by Eq. (16). Therefore, there are $N+2$ first-order differential equations which have to be solved simultaneously. In this case $N=5$ so that there are seven equations. The solution to the system of equations uses a fourth-order, Runge-Kutta method with an absolute accuracy of $10^{-6}$. Values of the efficiencies, sizes and terminal velocities are recomputed and updated at each time step (1.25 sec).

[1] Note that in Eq. (9) of Scott and Chen the last term should not be divided by the radius but the whole equation should be divided by the square of the radius.

Unauthenticated | Downloaded 06/25/24 06:41 PM UTC

TABLE 2. Comparison of the terminal velocities of small ice crystals and those of equivalent spheres.

| | | $\bar{R}$ (μm) | | | | | |
|---|---|---|---|---|---|---|---|
| | | 10 | | 20 | | 50 | |
| | | Columns | Disks | Columns | Disks | Columns | Disks |
| Density | (gm cm$^{-3}$) | 0.91 | 0.9 | 0.86 | 0.9 | 0.78 | 0.9 |
| Characteristic length $l$ or $d$ | (μm) | 24 | 20 | 49 | 48 | 127 | 156 |
| Best no. | | $6.7\times10^{-2}$ | 0.20 | 0.54 | 1.5 | 8.4 | 24.6 |
| Reynolds no. | | $1.1\times10^{-2}$ | $1.7\times10^{-2}$ | 0.13 | $9.8\times10^{-2}$ | 1.8 | 1.05 |
| Terminal velocity | (cm sec$^{-1}$) | 0.84 | 1.5 | 4.7 | 3.6 | 24.7 | 12.7 |
| Terminal velocity of an equivalent sphere | (cm sec$^{-1}$) | 0.76 | | 4.7 | | 24.7 | |

Kinematic viscosity $\nu=0.1772$.

## 10. Results

### *a. The general behavior of the solutions*

The solutions of the differential equations depend on the values chosen for the input parameters though the general trends of the solutions are not sensitive to these parameters. Hence, it is instructive to discuss this general behavior prior to dealing with specific parameters or specific clouds.

Fig. 4 presents the general behavior of the solutions. In this case the mass mean size $R$ of the precipitation particles increases as does their fall velocity $V$, as long as their electric charge $Q$ and the electric field $F$ are small. However, an increase in $V$ increases the charge separation and also increases the ambient electric field. As the electric field builds, the charge separation upon each collision increases. This positive feedback process causes a rapid increase in the electric field which starts at about point A on the figure. With the sudden increase in the electric field there is a strengthening of the electric force which opposes the fall of the precipitation elements since they carry negative charges. This decrease in velocity is significant in quenching the field buildup because the charge-generating term $\Sigma QV$ rapidly decreases [Eq. (14)]. As can be seen, the effect of the leakage current at this point is rather small and the decrease in $dF/dt$ is primarily due to the decrease in the generator term and the effect of diminished fall velocity. The process reaches equilibrium when the leakage current just equals the generator term. At that stage the relative velocities of the particles are small, the time rate of change of the field equals zero, and the electric field reaches a maximum.

The precipitation rate $p$ is determined by the particle sizes and terminal velocities [see Eq. (18)]. Thus, it is increased both by the increase in $R$ and increase in $V$ at the early stages of cloud development. However, at the later stages the greatly decreased velocity overcomes the effect of increasing size. Thus, if the electric field becomes large enough early enough, it is possible for sufficient rainwater to be levitated that a raingush will occur following a lightning stroke (see Levin and Ziv, 1974). The effect is illustrated in Fig. 5 where a cloud 2 km in diameter is considered with about 30-coulomb discharge with each lightning stroke and a field of 3.5 KV cm$^{-1}$ as a threshold value for the lightning discharge.

The discharge is simulated by removing an equal portion of the charge from each size interval. Here, as a result of the discharge, an increase in precipitation occurs which, in turn, results in further charge separation and further buildup of the electric field to a point at which precipitation almost stops and a new lightning stroke occurs. While the increase in precipitation rate described in the figure is smaller than the value observed by Moore *et al.* (1964), Levin and Ziv (1974)

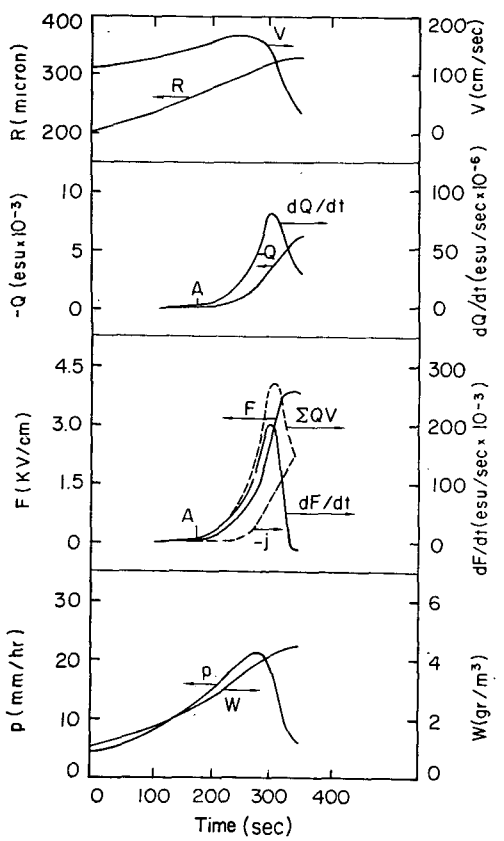


FIG. 4. General behavior of the solutions to the differential equations.

Unauthenticated | Downloaded 06/25/24 06:41 PM UTC

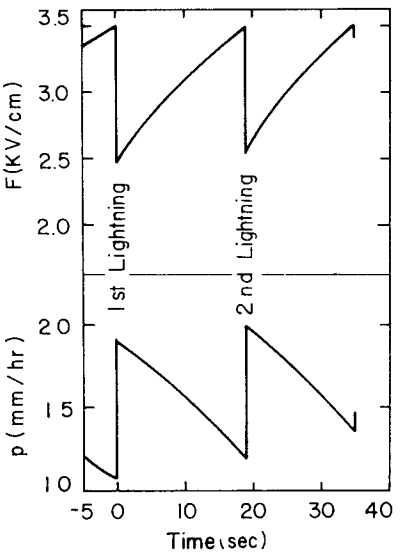


FIG. 5. Variation of the electric field and precipitation rate following lightning strokes in ice-water clouds with the parameters listed in Table 3.

have shown that this value can be considerably increased by an appropriate choice of particle size and amount of discharge.

*b. The point of charge reversal*

Fig. 6 shows the charge on the precipitation elements as a function of time. Initially, all precipitation particles acquire negative charges due to collisions with smaller uncharged cloud droplets. However, as the field builds up the polarization effect dominates and collisions between particles in intervals 3–5 with those in interval 2 result in transfer of large positive charge to the smaller particles. As a consequence, the charges in interval 2 change sign with time, and as the process persists more particles acquire positive charges. Since the fall velocities of these intermediate size particles is less than those of the larger particles in a real cloud, they would tend to be found at higher altitudes than the larger precipitation elements. This process may imply that the center of positive charge in the cloud increases in size and moves downward relative to the negatively charged precipitation elements.

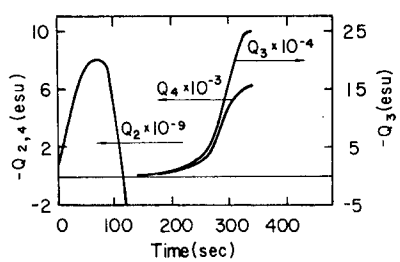


FIG. 6. Charge on the precipitation elements in size intervals 2, 3 and 4.

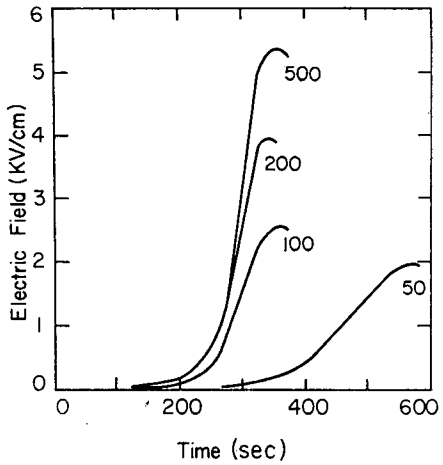


FIG. 7. Influence of the initial size of $R_4$ ($\mu$m) on the growth of the electric field. The initial liquid water content is 1 gm $m^{-3}$ in all cases.

*c. Changing the initial size of the particles*

Increasing the size of the cloud particles from 10 $\mu$m to either 20 or 50 $\mu$m while keeping the liquid water content constant does not affect appreciably the behavior of the field. For a given liquid water content, increasing the particle size decreases the number of particles. The effect of the decrease in collisions from this decrease in concentration is approximately compensated for by the increase in velocity. However, changing the initial value of $R_4$ has a profound effect (see Fig. 7). From the figure, it is seen that the field reaches its maximum value earlier and the maximum field strength attained is higher when the initial value of $R_4$ is increased. Two physical effects interact to produce this result—the size effect and the number effect. The larger the initial radius, the higher the terminal velocity which results in collisions and field buildup. However increasing the initial size of the precipitation particles for the same liquid water content reduces the concentration of the precipitation elements, thus reducing the number of collisions and the field buildup. The size effect is of greater importance because, as the size increases, the electric force needed to slow down the motion of the particles increases dramatically so that the maximum field is higher.

*d. The liquid water content*

Fig. 8 shows the effect of liquid water content on the behavior of the electric field. Reducing the initial water content of the precipitation delays the rapid buildup of the field (curve 2) but an even more pronounced delay occurs if the initial water content of the cloud drops is reduced. The effect of decreasing the initial quantity of precipitation is equivalent to starting the electrification process with a younger cloud or merely delaying the start of the rapid rise of the electric field.

Unauthenticated | Downloaded 06/25/24 06:41 PM UTC

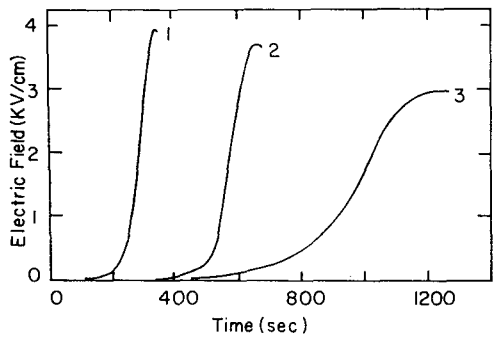


FIG. 8. The influence of the liquid water content in the cloud and in the precipitation particles on the growth of the electric field.

Curve 1: $W_c = W_p(0) = 1$ gm m$^{-3}$
Curve 2: $W_p(0) = 0.1$ gm m$^{-3}$, $W_c = 1$ gm m$^{-3}$
Curve 3: $W_p(0) = 1$ gm m$^{-3}$, $W_c = 0.1$ gm m$^{-3}$.

However, reducing the cloud-water content implies a reduced number of collisions, a reduced growth rate, and a reduced charge separation; hence, the greater delay in the awakening of the field.

*e. The efficiency of separation of charge*

Reduction of the efficiency of separation $E_3$ implies a lower charge generation rate without an effect on the growth of the hydrometeors. Comparing curve 2 with curves 3 and 4 of Fig. 9 we see that a reduction in the efficiency of charge generation results in a delay in the awakening of the field. But, surprisingly, since the hydrometeors have grown to a larger size at the time the field develops, a higher field is needed to stop their fall and hence a higher maximum value is finally attained. This means that, as a result of the highly nonlinear effects during the growth of the hydrometeors and the electric field, a less effective charging mechanism can actually generate a larger electric field. When ice particles are involved, the ratio $t_c/\tau$ of the contact time of the particles to the relaxation time of the ice becomes an important parameter. The ratio $t_c/\tau \to \infty$ when the particle is a conductor and then all the charge possible is transferred during a collision. However, if $t_c/\tau$ is unity only a portion (63%) of all the charge is transferred. In this case, comparing curve 3 to curve 2 of Fig. 9, we see that, again, a longer time is required for the buildup of the field and the final maximum value of electric field is higher. This fact becomes very important in fully glaciated clouds where the temperature is low (Sartor, 1970) and may explain the electrification of such clouds.

*f. Changing other parameters*

The initial value of the electric field, the fair weather value, does not affect the final maximum value of the electric field that can be attained provided the initial electric field is between 1 and 10 V cm$^{-1}$. Increasing

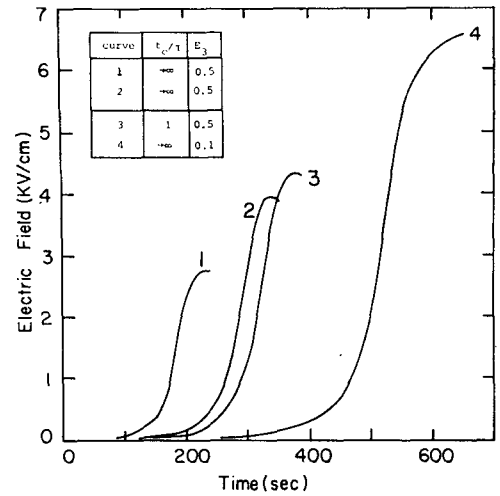


FIG. 9. Influence of the separation efficiency $E_3$ and the ratio $t_c/\tau$, of contact time to relaxation time, on the development of the electric field.

the effective collision angle $\theta$ between particles decreases the charging rate and results in an effect similar to decreasing the separation efficiency. Although changes in the effective density of particles to account for water drops, crystal shape, riming, etc., affect the fallspeeds of the particles, no significant change in the general behavior of the field occurs except perhaps to change the maximum field attained.

Since electrical effects are most prevalent in ice-water clouds, the properties of such clouds are used as a standard for comparison of the response of the other cloud types. In all the results presented thus far values appropriate for ice-water clouds are used. Table 3 presents the values of the parameters used for simulation of the different clouds. Of course, the response of the simulated cloud to different input parameters is related directly to the property of the cloud as a whole. In glaciated clouds one would expect: (i) the liquid water content to be lower than in ice-water clouds. (Hence, it

TABLE 3. Values of parameters used to simulate different cloud types.

| Parameter | Ice-water clouds | Ice-ice clouds | Water-water clouds |
|---|---|---|---|
| Liquid water content (gm m$^{-3}$) | $W_c = 1$ | $W_c = 0.1$–$0.2$ | $W_c = 1$ |
| | $\sum_{i=3}^{5} W_i = 1$ | $\sum_{i=3}^{5} W_i = 1$ | $\sum_{i=3}^{5} W_i = 1$ |
| Density (gm cm$^{-1}$) | $\rho_v = 1$ $\rho_p = 0.6$ | $\rho_c = \rho_p = 0.6$ | $\rho_c = \rho_p = 1$ |
| Separation efficiency | $E_3 = 0.5$ | $E_3 = 1$ | $E_3 \leqslant 0.1$ |
| Ratio of contact time to relaxation time | $t_c/\tau \to \infty$ | $t_c/\tau = 0.1$ | $t_c/\tau \to \infty$ |
| Average contact angle (deg) | $\theta = 45$ | $\theta = 45$ | $\theta = 45$ |
| Initial field (V cm$^{-1}$) | $F_0 = 5$ | $F_0 = 5$ | $F_0 = 5$ |
| Temperature (°K) | $T = 273$ | $T = 253$ | $T = 283$ |
| Pressure (mb) | 1013 | 700 | 1013 |

Unauthenticated | Downloaded 06/25/24 06:41 PM UTC

would be expected that a long time would be required to reach a high final field.); (ii) the efficiency of separation $E_3$ during collisions of ice crystals to be higher so that the field should reach a lower maximum at an earlier time; and (iii) the ratio $t_c/\tau$ to be lower.

The electrical behavior of clouds which contain only water differ from ice-water clouds in that the efficiency of separation should be low and the average angle of collision should be high.

Fig. 10 represents the calculated behavior of the electric field expected from the three cloud types with input parameters as listed in Table 3. The following conclusions are possible: In mixed clouds the electric field reaches a maximum value of 4 KV cm$^{-1}$ after about 5.5 min. The maximum precipitation rate is reached about 1 min prior to reaching the maximum field and has a value of about 19 mm hr$^{-1}$ (see Fig. 4). When the field is at its maximum the precipitation rate decreases dramatically to about 5 mm hr$^{-1}$ (see Fig. 4). In water-water clouds, the field growth is slow due to relatively small separation probability $E_3$ and to the large effective contact angle $\theta$. This implies a rapid growth of the drops and a rapid growth of the precipitation rate. When the electric field reaches only 65 V cm$^{-1}$ (see Fig. 10) after about 600 sec the precipitation rate reaches the unreasonable high value of 140 mm hr$^{-1}$. It keeps growing rapidly with time and reaches a value of about 250 mm hr$^{-1}$ after about 750 sec when the field is about 1 KV cm$^{-1}$. These high precipitation rates may be a result of the constant $W_c$ A more sophisticated model which includes the vertical dimension as well as the time may be able to resolve this difficulty. However, it is believed that high precipitation rates will also occur since the relatively low efficiency of separation does not permit the rapid growth of the electrical forces. Hence, when the precipitation rate is high the cloud develops a downdraft, it decays, and no further significant electrification occurs. Hence it may be concluded that lightning from warm clouds is improbable unless there are extremely high precipitation rates.

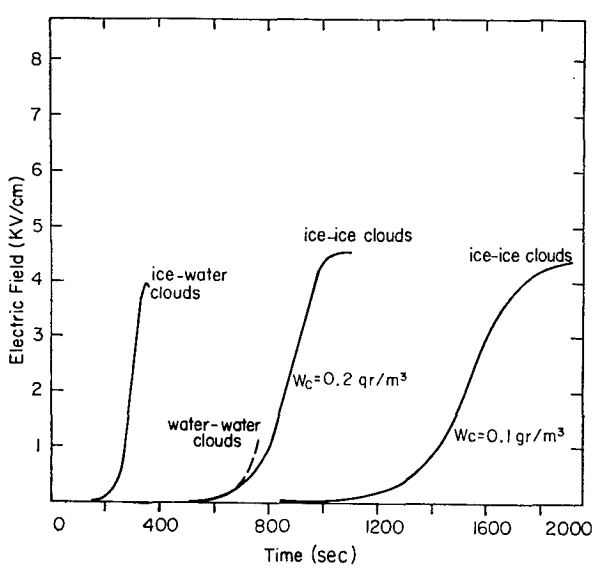


FIG. 10. Behavior of the electric field in different thunderclouds.

In fully glaciated clouds the behavior of the electric field strongly depends on the liquid water content. With a liquid water content of 0.2 gm m$^{-3}$ a maximum field of 4.6 KV cm$^{-1}$ is reached after less than 20 min, while $W_c=0.1$ gm m$^{-3}$ the same maximum is reached after 30 min. In both cases the precipitation rate is realistic.

Therefore, it is expected that electric fields of a few KV cm$^{-1}$ are possible in mixed clouds which develop within 5–6 min. Such fields can also develop in ice-ice clouds if there is sufficient equivalent liquid water content or the cloud lifetime is sufficient. High electric fields in warm clouds are improbable.

The effect of relaxation time during ice-ice interactions is important and should be emphasized. It has been argued that short contact times result in small charge separation which is not sufficient to generate high electric fields. This work suggests that if the ratio $t_c/\tau$ is small and small charges are transferred with each collision, the maximum electric field attained will be higher. As mentioned earlier, the maximum electric field is limited not by the charge transferred per collision but by the size of the precipitation particles and their relative fallspeed. Larger ice particles produce a larger maximum electric field because they are not easily levitated.

## 11. Summary

This study of the growth of the electric field in thunderclouds utilizes a time-dependent numerical model which simultaneously follows the growth of the hydrometeors and their electrical charge. The results clearly demonstrate the close coupling between the growth of the cloud and its electrical state. Clouds containing large ice particles and small drops are found to be the most favorable for the growth of the electric field to values which produce lightning. Fully glaciated clouds also may generate lightning but probably require more time. Warm clouds, on the other hand, normally do not generate high fields and seldom produce lightning.

## APPENDIX

### Computation of the Fall Velocities

The terminal velocities are computed by considering drag, gravity and electrical forces. It is assumed that enough time passes between collisions so that accelerations of the particles can be neglected. The appropriate equation of motion for a particle is

$$\frac{d^2Z}{dt^2}=M'g+QF-D, \qquad \text{(A1)}$$

where $M$ is the effective mass of the particle which in-

Unauthenticated | Downloaded 06/25/24 06:41 PM UTC

cludes buoyancy effects, $g$ the acceleration due to gravity, $Q$ the charge on the particle, $F$ the ambient electric field, and $D$ the drag forces. At terminal velocity

$$D=M'g+QF, \tag{A2}$$

where $D$ is given by

$$D=\tfrac{1}{2}AC_D\rho_aV^2, \tag{A3}$$

and $A$ is the particle's cross section.

Using the definitions of the Reynolds number (Re) and Best number (X) for a sphere, we have

$$\mathrm{X}=C_D\mathrm{Re}^2=C_DR^2V^2\rho_a\frac{4\rho_a}{\eta^2}, \tag{A4}$$

$$C_DR^2V^2\rho_a=\frac{\mathrm{X}\eta^2}{4\rho_a}. \tag{A5}$$

Substituting (A5) into (A3), we have

$$D=\frac{\pi}{2}\frac{\mathrm{X}\eta^2}{4\rho_a}, \tag{A6}$$

and, since

$$M'=\tfrac{4}{3}\pi R^3(\rho-\rho_a), \tag{A7}$$

Eq. (A2) becomes

$$\mathrm{X}=\frac{32}{3}\frac{\rho_a(\rho-\rho_a)g}{\eta}R^3+\frac{8\rho_a}{\pi\eta^2}QF. \tag{A8}$$

This relation is independent of $V$ or $C_D$ and allows the explicit calculation of X knowing $Q$, $\rho$ and $R$ of the particle, and $\eta$, $\rho_a$ and $F$ of the environment. Final solution is provided by considering the explicit empirical relation given by Davies (1945) which allows a direct calculation of Re knowing X. The calculated values of terminal velocity show a maximum error of only 3% when compared with Gunn and Kinzer (1948). Davies' equations are:

For $\mathrm{X}<120$

$$\mathrm{Re}=\mathrm{X}/24-2.3363\times10^{-4}\mathrm{X}^2+2.05\times10^{-6}\mathrm{X}^3-6.9105\times10^{-9}\mathrm{X}^4 \tag{A9}$$

For $\mathrm{X}>120$

$$\log\mathrm{Re}=-1.29536+0.986(\log\mathrm{X})-4.6677\times10^{-2}(\log\mathrm{X})^2+1.1235\times10^{-3}(\log\mathrm{X})^3 \tag{A10}$$

The value of Re is then used to evaluate the terminal velocity $V$:

$$V=\frac{\mathrm{Re}\eta}{2\rho_aR}. \tag{A11}$$

The more recent work of Beard and Pruppacher (1969) was not used for the evaluation of the terminal velocities because of the longer computer time; our values deviate by less than 2% from those of Beard and Pruppacher.

## REFERENCES


Aufdermaur, A. N., and D. A. Johnson, 1972: Charge separation due to riming in an electric field. *Quart. J. Roy. Meteor. Soc.*, **98**, 369–382.

Beard, K. V. and H. R. Pruppacher, 1969: A determination of the terminal velocity and drag of small water drops by means of a wind tunnel. *J. Atmos. Sci.*, **26**, 1066–1072.

Berry, E. X, 1967: Cloud droplet growth by collection. *J. Atmos. Sci.*, **24**, 688–701.

Davies, C. N., 1945: Definitive equations for the fluid resistance of spheres. *Proc. Phys. Soc. London*, **57**, 259–270.

Davis, M. H., 1964: Two charged spherical conductors in a uniform electric field: forces and field strength. *Quart. J. Mech. Appl. Math.*, **17**, 499–511.

——, and J. D. Sartor, 1967: Theoretical collision efficiencies for small cloud droplets in strokes flow. *Nature*, **215**, 1371–1372.

Golovin, A. M., 1963: The solution of the coagulation equation for cloud droplets in a rising air current. *Bull. Acad. Sci. USSR Geophys. Ser.*, No. 5, 482–487.

Gunn, R., and G. D. Kinzer, 1949: The terminal velocity of fall for water droplets in stagnant air. *J. Meteor.*, **6**, 243–248.

Heymsfield, A., 1972: Ice crystal terminal velocities. *J. Atmos. Sci.*, **29**, 1348–1357.

Kovetz, A., and B. Olund, 1969: The effect of coalescence and condensation on rain formation in a cloud of finite vertical extent. *J. Atmos. Sci.*, **26**, 1060–1065.

Latham, J., and B. J. Mason, 1962: Electrical charging of hail pellets in a polarizing electric field. *Proc. Roy. Soc. London*, **A266**, 387–401.

Levin, Z., and P. V. Hobbs, 1971: Splashing of water drops on solid and wetted surfaces: hydrodynamics and charge separation. *Phil. Trans. Roy. Soc. London*, **269A**, 555–585.

——, and A. Ziv, 1974: The electrification of thunderclouds and the rain gush. *J. Geophys. Res.*, **79** (in press).

Mason, B. J., 1971: *The Physics of Clouds*. London, Oxford University Press, 521–557.

——, 1972: The physics of thunderstorm. *Proc. Roy. Soc. London*, **A327**, 433–466.

Moore, C. B., B. Vonnegut, E. A. Vrablik and D. A. McCraig, 1964: Gushes of rain and hail after lightning. *J. Atmos. Sci.*, **21**, 646–665.

Paluch, I. R., and J. D. Sartor, 1973: Thunderstorm electrification by the inductive charging mechanism: I. Particle charges and electric fields. *J. Atmos. Sci.*, **30**, 1166–1173.

Sartor, J. D., 1967: The role of particle interactions in the distribution of electricity in thunderstorms. *J. Atmos. Sci.*, **24**, 601–615.

——, 1970: General thunderstorm electrification. NCAR, Boulder, Colo.

Scott, W. D., and Z. Levin, 1970: The effect of potential gradient on the charge separation during interaction of snow crystals with an ice sphere. *J. Atmos. Sci.*, **27**, 463–473.

Scott, W. T., 1968: Analytic studies of cloud droplet coalescence I. *J. Atmos. Sci.*, **25**, 54–65.

——, and C. Y. Chen, 1970: Approximate formulas fitted to the Davis-Sartor-Shafrir-Neiburger droplet collision efficiency calculation. *J. Atmos. Sci.*, **27**, 698–700.

Slinn, W. G. N., and A. G. Gibbs, 1971: The stochastic growth of a rain droplet. *J. Atmos. Sci.*, **28**, 973–982.

Twomey, S., 1966: Computation of rain formation by coalescence. *J. Atmos. Sci.*, **23**, 405–411.

Warshaw, M., 1967: Cloud droplet coalescence: Statistical foundations and a one-dimensional sedimentation model. *J. Atmos. Sci.*, **24**, 278–286.

——, 1968: Cloud droplet coalescence: Effects of the Davis-Sartor collision efficiency. *J. Atmos Sci.*, **25**, 874–877.

Whelpdale, D. M., and R. List, 1971: The coalescence process in raindrop growth. *J. Geophys. Res.*, **76**, 2836–2856.


Unauthenticated | Downloaded 06/25/24 06:41 PM UTC